

## Article

# Synthesis of New Modified with Rhodamine B Peptides for Antiviral Protection of Textile Materials

Petar Todorov <sup>1,\*</sup>, Stela Georgieva <sup>2</sup>, Desislava Staneva <sup>3</sup>, Petia Peneva <sup>1</sup>, Petar Grozdanov <sup>4</sup>, Ivanka Nikolova <sup>4</sup> and Ivo Grabchev <sup>5</sup>

<sup>1</sup> Department of Organic Chemistry, University of Chemical Technology and Metallurgy, 1756 Sofia, Bulgaria; petenceto\_2@abv.bg

<sup>2</sup> Department of Analytical Chemistry, University of Chemical Technology and Metallurgy, 1756 Sofia, Bulgaria; st.georgieva@uctm.edu

<sup>3</sup> Department of Textile and Leathers, University of Chemical Technology and Metallurgy, 1756 Sofia, Bulgaria; grabcheva@mail.bg

<sup>4</sup> The Stephan Angeloff Institute of Microbiology, Bulgarian Academy of Sciences, 1113 Sofia, Bulgaria; grozdanov@microbio.bas.bg (P.G.); inikolova@microbio.bas.bg (I.N.)

<sup>5</sup> Faculty of Medicine, Sofia University "St. Kl. Ohridski", 1407 Sofia, Bulgaria; i.grabchev@chem.uni-sofia.bg

\* Correspondence: pepi\_37@abv.bg; Tel.: +359-2-8163423

**Abstract:** Here we report on the synthesis and characterization of three new N-modified analogues of hemorphin-4 with rhodamine B. Modified with chloroacetyl, chloride cotton fabric has been dyed and color coordinates of the obtained textile materials were determined. Antiviral and virucidal activities of both the peptide-rhodamine B compounds and the dyed textile material were studied. Basic physicochemical properties (acid-base behavior, solvent influence, kinetics) related to the elucidation of structural activity of the new modified peptides based on their steric open/closed ring effect were studied. The obtained results lead to the conclusion that in protic solvent with change in pH of the environment, direct control over the dyeing of textiles can be achieved. Both the new hybrid peptide compounds and the modification of functionalized textile materials with these bioactive hemorphins showed virucidal activity against the human respiratory syncytial virus (HRSV-S2) and human adenovirus serotype 5 (HAdV-5) for different time intervals (30 and 60 min) and the most active compound was Rh-3.

**Keywords:** rhodamine-peptides; hemorphins; cotton fabric; absorbance; emission; virucidal effect; antiviral activity



**Citation:** Todorov, P.; Georgieva, S.; Staneva, D.; Peneva, P.; Grozdanov, P.; Nikolova, I.; Grabchev, I. Synthesis of New Modified with Rhodamine B Peptides for Antiviral Protection of Textile Materials. *Molecules* **2021**, *26*, 6608. <https://doi.org/10.3390/molecules26216608>

Academic Editors: Hiroyuki Konno and Kenichi Akaji

Received: 15 October 2021

Accepted: 29 October 2021

Published: 31 October 2021

**Publisher's Note:** MDPI stays neutral with regard to jurisdictional claims in published maps and institutional affiliations.



**Copyright:** © 2021 by the authors. Licensee MDPI, Basel, Switzerland. This article is an open access article distributed under the terms and conditions of the Creative Commons Attribution (CC BY) license (<https://creativecommons.org/licenses/by/4.0/>).

## 1. Introduction

The xanthene dyes are widely used in medicinal and bioorganic chemistry as biologically active compounds (either alone or conjugated). These compounds possess potent antiviral activity against a human foreskin fibroblast (vesicular stomatitis virus) and enhance the antiviral activity of xanthene derivatives from 8- to 15-fold [1]. Rhodamine B derivatives represent an important tool for studies of more complex biochemical processes and activities. Such kind of fluorescence-based probes of bioactive molecules possess desirable features; they have an excellent spectral characteristics and relatively facile syntheses [2,3]. Moreover, rhodamine B and its derivatives do not have a cytotoxic effect [4]. It is inexpensive, resistant under a variety of reaction conditions, can be covalently linked to bioactive molecules such as peptides, and has suitable spectral properties in terms of absorption and fluorescence wavelength. Rhodamine B is a lipophilic cation belonging to the family of xanthenes, and its derivatives are widely employed as fluorophore probes [3,5]. It is known that they are sensitive as fluorescent turn-on compounds. The only drawback to the use of rhodamine B is the formation of a spirolactam compound, which is non-fluorescent and cannot be used for all fluorescent microscopic applications [6].

Recently, a new class of rhodamine derivatives displaying a broad-spectrum antiviral activity against different enveloped viruses including an HSV-2 acyclovir resistant strain has been reported [7]. Unfortunately, many viral infections are the cause of death worldwide, and still now there are no efficient antiviral drugs or vaccines for a large number of viruses, and this represents a great challenge especially for emerging and re-emerging viral diseases [7]. Moreover, the peptides and peptide-conjugated molecules, having a propensity to interact with membrane interfaces, might exert broad antiviral activity against enveloped viruses. [8].

The peptides can be useful as substituents of the proteins, especially when site-specific modification of the required protein is difficult or impractical. Peptides are sufficiently small molecules which can be easily modified in the laboratory using standard synthetic protocols and solid-phase peptide (SPPS) methods. The large part of peptides can play role of ligands, since they contain a significant number of precisely located functional groups and amino acid residues, which possess high-affinity and specific interactions with a target receptor. This is usually harder to achieve with small molecules [9,10]. The peptide scaffolds allow the introduction of fluorophores in their structure while retaining the biological activity, which can increase the possibilities for the design of fluorescent sensors and their applications in biochemistry and medicine [11,12]. This kind of fluorophore molecule is incorporated into or appended to a known peptide sequence that has high affinity for the target protein. The presence of amino acid residues that have both aromatic moiety and hydrophobic nature, such as Trp, Phe, and Tyr, favor protein binding. Replacement of this residue with fluorophore provides a significant change in protein binding and a correspondingly strong enhancement of the fluorescence signal [9].

Hemorphins are endogenous peptides, belonging to the family of atypical opioid peptides, released during the sequential cleavage of hemoglobin proteins [13–15]. Hemorphins have been shown to exhibit diverse therapeutic effects in both human and animal models [16–18]. Hemorphin-4 (Tyr-Pro-Trp-Thr) is a member of the hemorphins family, an endogenous nonclassical opioid peptides derived from hemoglobin. There is evidence that these kinds of natural or synthetic tetrapeptides exert opioid activities *in vivo* and, therefore, may play an important physiological role [19]. Our previously investigations have demonstrated that not only the position of modification, but also the nature of the incorporated group, lead to significant changes in the peptide activity and affinity [20–25]. Recently, the rhodamine B-labelled arginine-rich peptide has been designed as the heparin bioreceptor to construct a highly sensitive and selective fluorescent biosensor for heparin detection [26]. However, there are no data in the literature concerning rhodamine conjugated hemorphin analogues.

A recent study has reported that the hemorphins bind with high affinity to angiotensin-converting enzyme (ACE) [27]. ACE2 is expressed in nearly all human organs in varying degrees. Both SARS-CoV-2 and SARS-CoV enter host cells via the angiotensin-converting enzyme 2 (ACE2) receptor [28]. Thus, targeting the ACE2 receptor of host cells can block the entry of the virus into the cell, thereby protecting the host from viral infection and pandemic disease COVID-19 [29].

Different methods of textile materials functionalization exist in order to achieve biologically-active effects. Most of these methods/reagents are controversial for humans and the environment due to inorganic salts, phenols and thiophenols, antibiotics, formaldehyde derivatives, etc. which are used during production [30]. Therefore, the development of new methods has to fulfil the requirements of being safe for both human health and the environment. In conjunction with such functionalization, there is a question concerning to which extent the normal skin flora of healthy people will be destroyed by action of an antimicrobial compound [31]. Therefore, the increasing tendency of research is seen where the functionalization is performed by the use of non-toxic, biodegradable, and environmentally-friendly reagents. Currently, the peptides are the candidate therapeutic agents that offer selectivity and specificity, and low levels of side effects. The great advantage of peptides against viruses consists in the reduced possibility of developing re-

sistance during the treatment [32]. Cotton has widespread use in textiles and in healthcare environments. Peptides can be simply adsorbed on cotton through electrostatic interactions but without covalent bonding they are easily lost. Functionalization of cotton can impart suitable groups for covalent bonding of different polymers and ensure durability of modification during use [33].

Herein we report on the synthesis and characterization of new N-modified analogues of hemorphin-4 with rhodamine B. We have also investigated the modification of the functionalized cotton fabric with the new hybrid peptide compounds. The potential antiviral and virucidal activities of both peptides and textiles material have also been studied.

## 2. Results and Discussion

### 2.1. Chemistry

We have synthesized and characterized new rhodamine B-conjugated hemorphin-4 analogues as a potential sensitive fluorescent probe for color, antiviral, and virucidal activity of textile materials. These peptides contain different aliphatic amino acid residue and differed by the increased number of methylene group (from one to three) between rhodamine B moiety to the N-side and the amino acid scaffold of natural hemorphin-4. The aim of this study was to determine evidence of the significance of different amino alkyl residues of newly synthesized hybrid compounds for their physicochemical properties and to investigate their structurally-related properties and potential textile applications using different methods. We have also explored an approach to the structural features of pH-dependent equilibrium between the spirolactam form and the ring-opened form of these peptides, the potential antiviral and virucidal activities of both of the new hybrid peptide molecules, and the modification of functionalized cotton fabrics with these bioactive hemorphins.

RhodamineB-Gly-Tyr-Pro-Trp-Thr-NH<sub>2</sub> (Rh-1), rhodamineB-β-Ala-Tyr-Pro-Trp-Thr-NH<sub>2</sub> (Rh-2), and rhodamineB-γ-Abu-Tyr-Pro-Trp-Thr-NH<sub>2</sub> (Rh-3) were efficiently prepared via solid-phase peptide synthesis (SPPS) using Fmoc (9-fluorenylmethoxy-carbonyl) chemistry. This strategy, based on the reaction between rhodamine-B with the N-terminal amino group of the hemorphin-4 analogues, was applied directly to the resin. The synthetic route is summarized in Figure 1. In order to achieve peptide bond formation and to improve the efficiency of peptide synthesis, the organic compounds such as TBTU (2-(1H-benzotriazole-1-yl)-1,1,3,3-tetramethylaminium tetrafluoroborate) and HOBt (hydroxybenzotriazole) as coupling reagents, and DIPEA (N,N-diisopropylethyl-amine) as an organic base were added to reaction media in each step. After cleavage of the product from Rink-Amide MBHA Resin, the compounds were purified from crude product by semi-preparative HPLC with a C18 column. The Mass spectra confirmed the spirolactam form of peptides formation.

The handling of the amino acidic scaffold can be regarded as a potentially powerful tool in both bioorganic and medicinal chemistry investigations and the development of new drugs and materials [34].

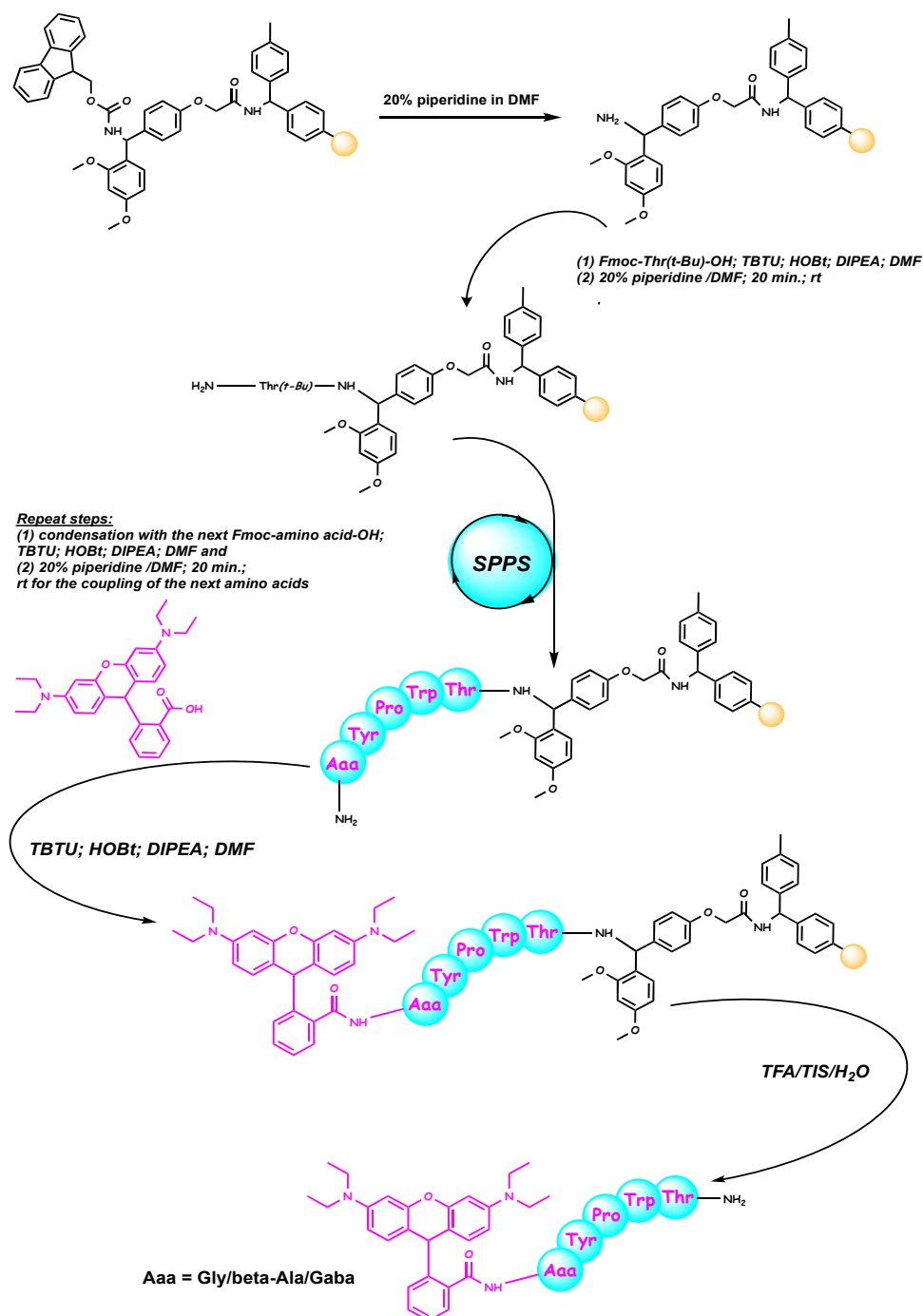


**Figure 1.** Schematic representation of the solid phase synthesis of the new hybrid peptides.

## 2.2. Physicochemical Characterizations

### Determination of Physicochemical Constants

The values of the dissociation constants of the test compounds were determined using potentiometric titration. The calculated values are important for the direct application of the compounds in the process of their bonding to the textile material. It is known that one of the most important physical and chemical factors of micro- and macromolecules is the value of the acid dissociation constant (pK), used to determine the type of individual protonated and unprotonated forms of compounds and to measure the strength of acids and bases. Basically, the physicochemical properties of the compounds depend on the pH of the medium. This parameter is an important factor in the dyeing process and the interaction of

the dye with the textile material. After data processing from the titration, the dissociation constants of the compounds were determined by the Hassenbach equation [23,24]. From Figure 2 it can be seen that rhodamines are referred to as diprotic acids, dissociating gradually. The calculated values of pKa and pI are summarized in Table 1. The values of the dissociation constants of the three rhodamine derivatives are approximately equal but can still be arranged in the following sequence:  $pK_1(\text{Rh-2}) < pK_1(\text{Rh-1}) < pK_1(\text{Rh-3})$ . Since the pKa of Rhodamine B defines the equilibrium between the spirocyclic form and the ring-opened form, it can be reasoned that the pKa values of rhodamines could be modulated by introducing different amino acid residues of the peptide chain. pH-dependent equilibrium between the spirocyclic form and the ring-opened form of Rh-1, Rh-2, and Rh-3 are shown in Figure 3. As mentioned, compounds 1 and 2 have a slightly lower value than 3, which may be due to the closer proximity of the hydroxy group of Tyr to the spirocyclic carbon, where the steric effect may be more pronounced. The calculated values of the isoelectric points show that in a weakly acidic medium (pH~4) the compounds will have zero charges (neutrality of the molecule) and, accordingly, insolubility which was taken into account at the textile dyeing.

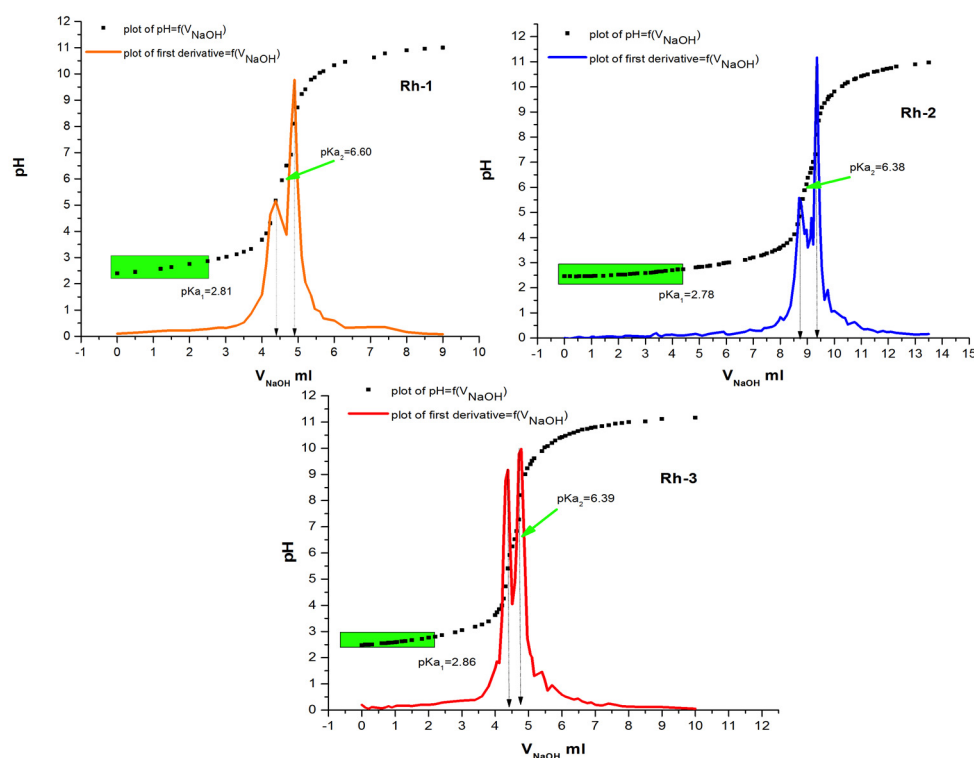


**Figure 2.** Plot of pH vs.  $V_{\text{NaOH}}$  and first derivatives graphics of 20  $\mu\text{mol}$  of Rh-1, Rh-2, and Rh-3, respectively.

**Table 1.** Physicochemical characterization of Rh-1, Rh-2, and Rh-3.

Compound	pK		pI	k, $\text{s}^{-1}$	$\tau_{1/2}$
	pK <sub>1</sub>	pK <sub>2</sub>			
Rh-1	2.81	6.6	4.7	$4.65 \times 10^{-2} \pm 0.0046$	14.9
Rh-2	2.78	6.38	4.58	$5.53 \times 10^{-2} \pm 0.0012$	12.5
Rh-3	2.86	6.39	4.63	$8.12 \times 10^{-2} \pm 0.0014$	8.54

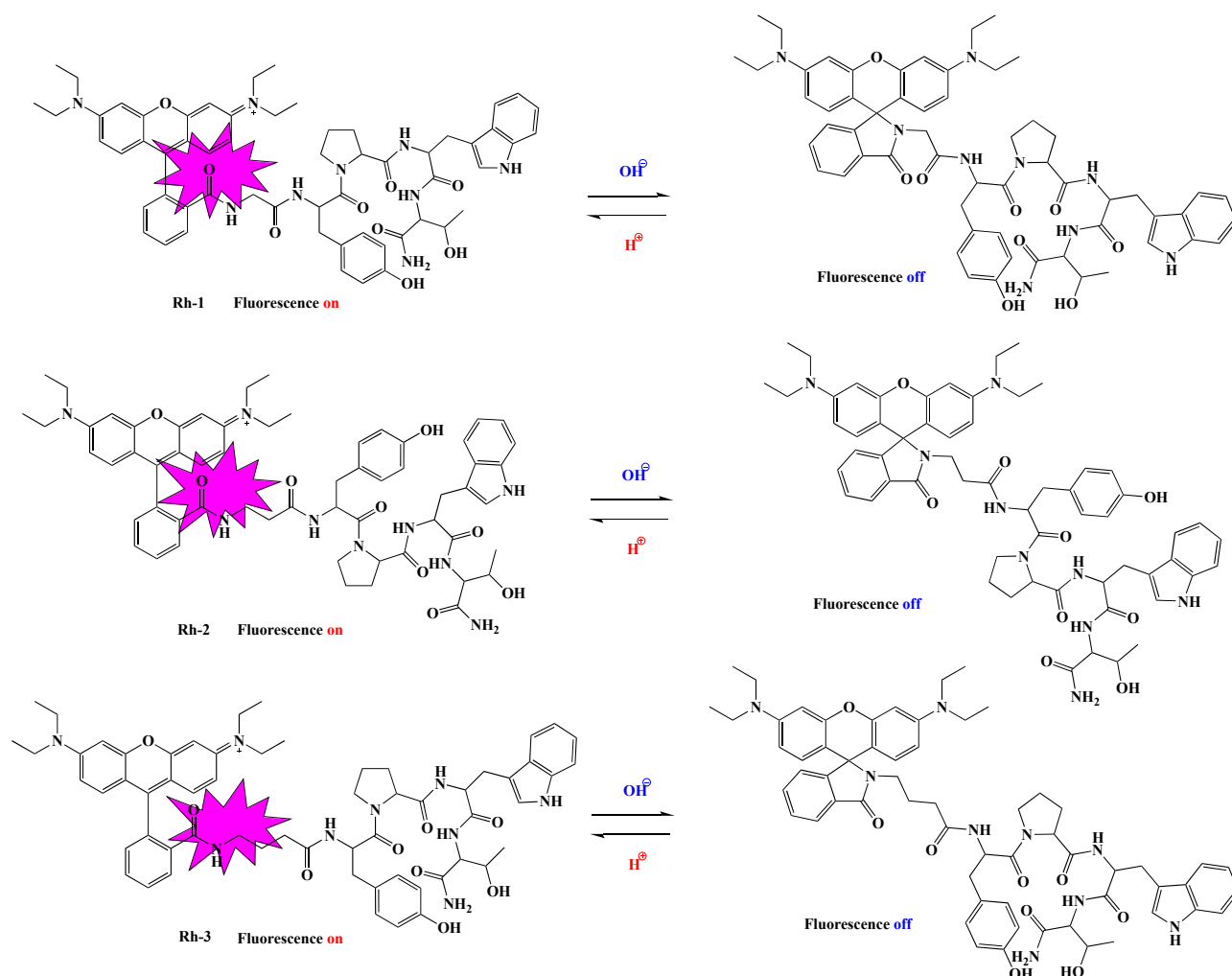


**Figure 3.** pH-dependent equilibrium between the spirolactam form and the ring-opened form of rhodamine B-conjugated hemorphin-4 analogues.

### 2.3. Spectral Characterizations

The new compounds were characterized by FT-IR, UV-Vis, and fluorescence spectroscopy in two types of solvents (water (polar protic solvent) and triethylamine (polar aprotic solvent)) in order to investigate changes in the color of the solution directly related to the structure of the compounds. The spectra related to the absorption of electromagnetic radiation of the rhodamine derivatives are given in Figure 4. Two well-formed absorption peaks with different intensity in both used solvents, localized at  $\lambda_{\text{max}} \approx 230$ ,  $\approx 278$  nm and 561 nm in the water solutions and  $\lambda_{\text{max}} \approx 300$  nm and 565 nm of solution of triethylamine, respectively, can be seen (Figure 4). Basically, the  $\pi \rightarrow \pi^*$  transitions of the  $> \text{C}=\text{O}$  in the peptide bonds is occurred by UV absorption of the peptide molecule in the range 180 to 230 nm. The aromatic side-chains of indole of Trp, phenol rings of Tyr, and rhodamine are primarily responsible for absorption of the  $\pi$ -electron systems of aromatic groups in the range of  $\approx 300$  nm [35,36]. The absorption bands occurring at this wavelength are equally intense due to the same number of peptide bonds and the concentration of analyzed solutions. The studied dependence on the pH of the water medium showed that the colors of the aqueous solutions remain unchanged from the strongly acidic medium in which they dissolve to the strongly alkaline one. There is a visible change in the hue of the solutions for the individual compounds, but the difference in the wavelength at which the compounds absorb in the visible region is minimal (2–5 nm). The studied dependence on the pH of the water medium showed that the colors of the aqueous solutions remain unchanged from

the strongly acidic medium to the strongly alkaline one. The absorption peak intensity increased three-fold with the decrease of pH values from 12 to 1 (Figures 4 and 5).

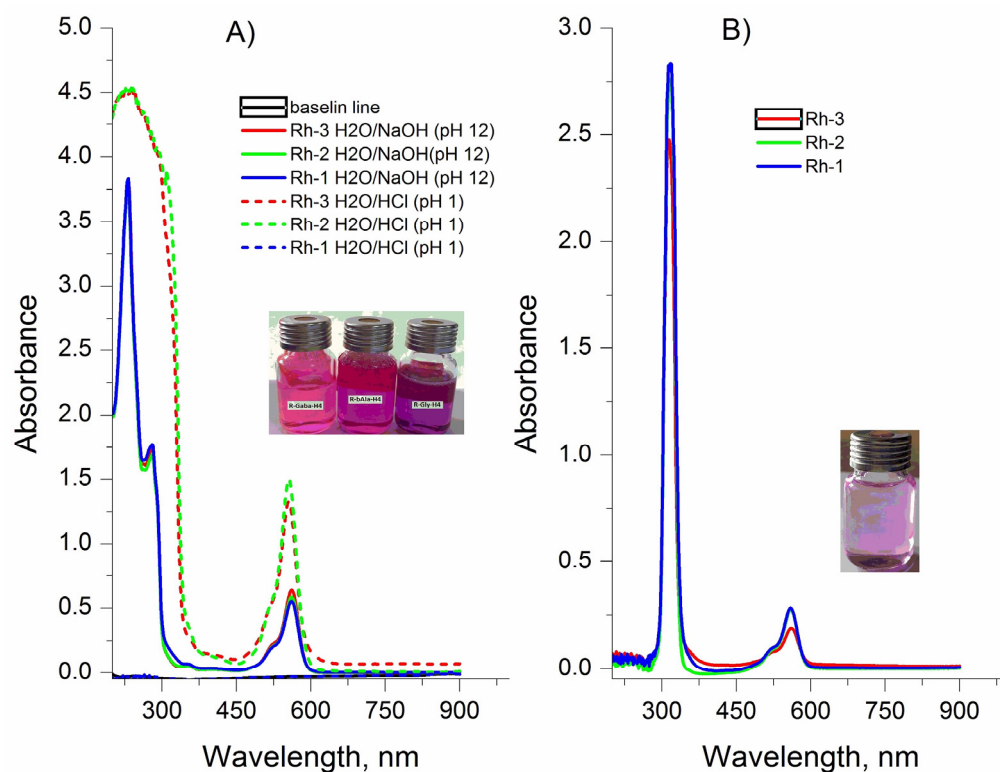


**Figure 4.** UV-Vis spectrum of Rhodamine derivatives at: (A) equal concentration of the compounds and different pH of solutions. Absorbance of the solution was measured against water; (B) solutions of Rh-1, Rh-2 and Rh-3 in triethylamine with equal concentration of the compounds. Absorbance of the solution was measured against triethylamine.

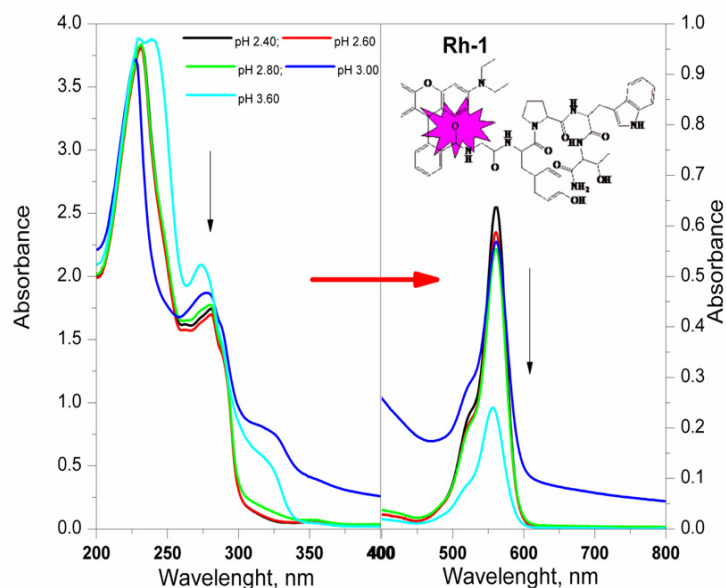


**Figure 5.** Uv-Vis spectrum of Rh-1 ( $4.09 \times 10^{-5}$  mol L<sup>-1</sup>) at different pH.

A similar property of rhodamine-related peptides was observed by Meng-Chan Xia et al. [37]. Color stability was observed in the aqueous solutions of the compounds, although the intensity of the absorption maxima depended on the pH of the medium. The molar extinction coefficients

in the long-wavelength absorption maximum are, respectively, Rh-3 ( $\epsilon = 1.83 \times 10^4 \text{ cm.mol.L}^{-1}$ ); Rh-1 ( $\epsilon = 2.04 \times 10^4 \text{ cm.mol.L}^{-1}$ ); and Rh-2 ( $\epsilon = 2.16 \times 10^4 \text{ cm.mol.L}^{-1}$ ). The behavior of the compounds in an aprotic solution of triethylamine is different. For about 6–120 min, a visible fading of the solution is observed until the complete disappearance of the color. This is due to the observed steric effect in the molecules of the compounds associated with the case of spirolactam ring opening. This provoked our interest in studying, in addition, the influence of the environment on the structural changes of the compounds. The effect of the peptide substituent on the ring opening/closing time is clearly visible with studying the kinetics of the process. For this purpose, the spectra of the solution were taken at the initial moment, immediately after its preparation and subsequently on every 5–10 min. Figure 6 shows the decrease in the intensity of the absorption peak. The kinetic lines were taken at the same time interval and by fluorescence (Figure 7). The observed small Stokes shift is typical for rhodamine dyes. It is characteristic and of the newly synthesized rhodamine B-conjugated hemorphin-4 analogues. However, the increase in the spacer length between chromophore and peptides leads to a minor enhancement of Stokes shift due to the changes in molecule mobility [5,38].

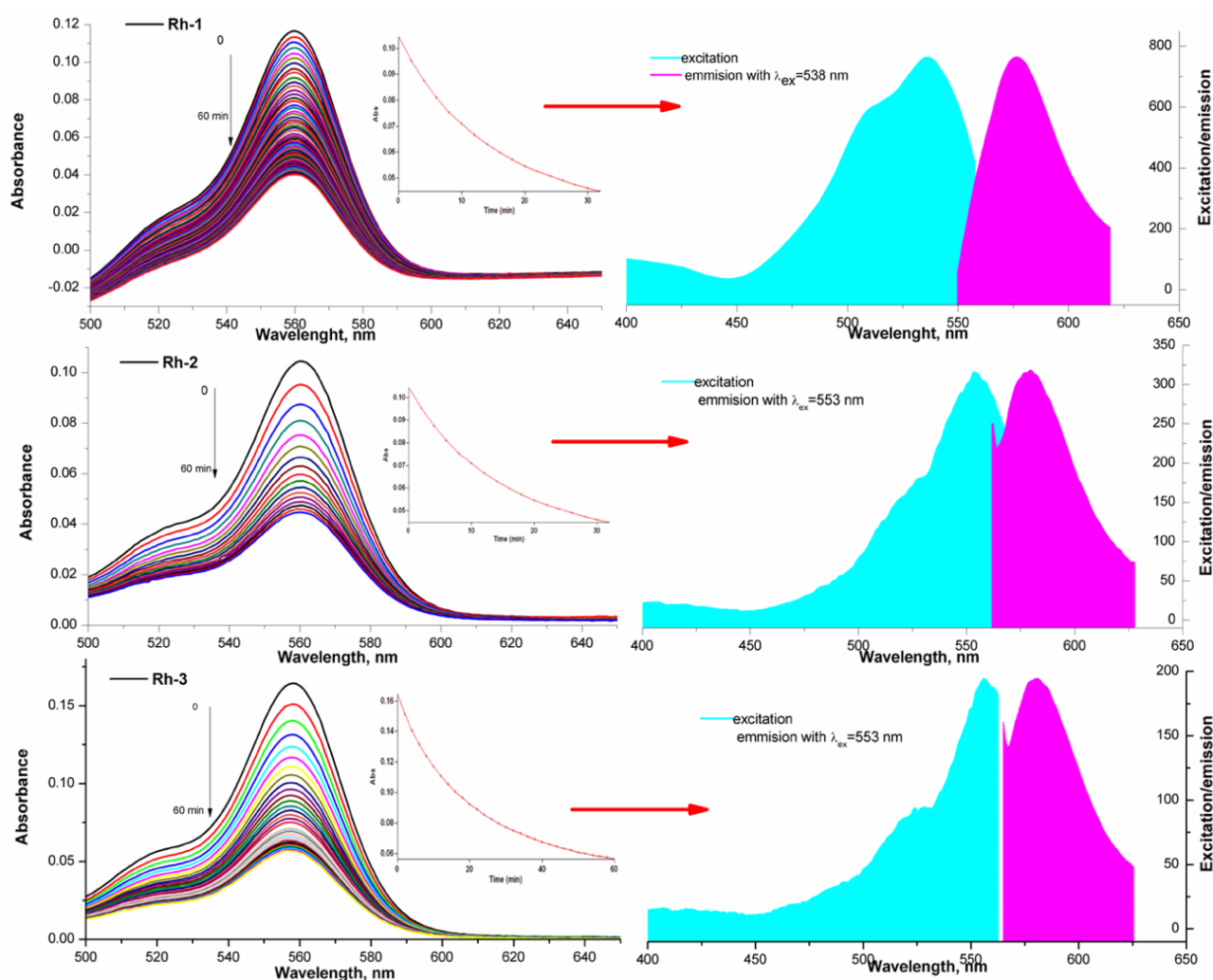


**Figure 6.** Uv-Vis kinetic plot of the first-order reaction between ring-opened and formed of the spirolactam form at equal concentration of Rh-1, Rh-2, and Rh-3 (at 25 °C) and corresponding fluorescence spectra in aprotic solvent (triethylamine). Rh-1  $\lambda_{abs}$  (nm): 565,  $\lambda_{em}$  (nm): 589, Stokes shift ( $\text{cm}^{-1}$ ): 721; Rh-2  $\lambda_{abs}$  (nm): 561,  $\lambda_{em}$  (nm): 593, Stokes shift ( $\text{cm}^{-1}$ ): 962; Rh-3  $\lambda_{abs}$  (nm): 559,  $\lambda_{em}$  (nm): 592, Stokes shift ( $\text{cm}^{-1}$ ): 997.

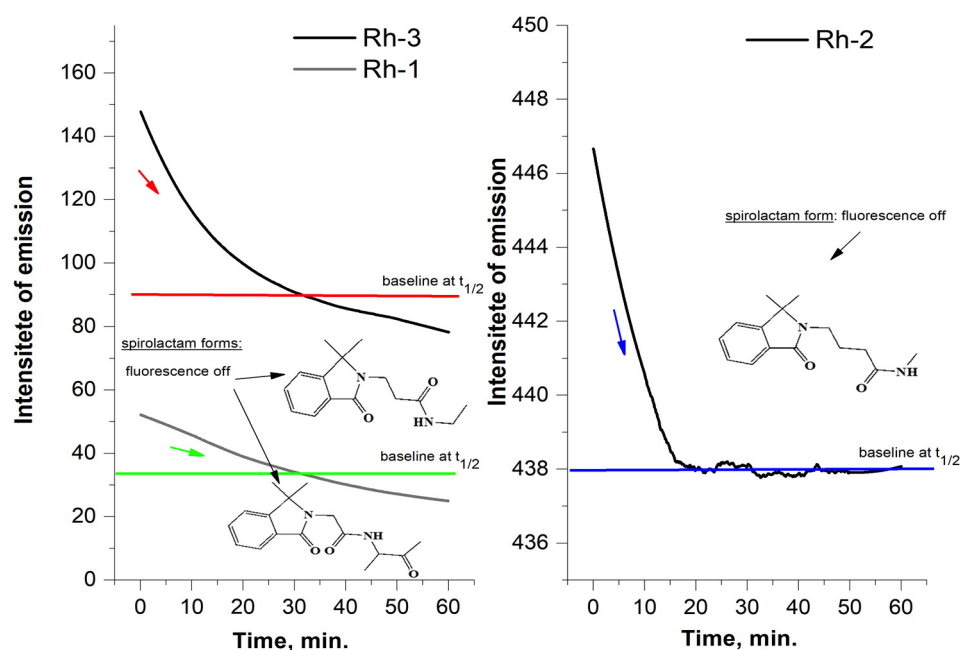


**Figure 7.** Fluorescence kinetic plot of the first-order reaction between ring-opened and formed of the spirolactam form at equal concentration of Rh-1, Rh-2 and Rh-3 and 25 °C.

From a thermodynamic point of view, the opening/closing reaction of the spirolactam ring is a first-order reaction [36]. The kinetic law with respect to the exhaustion of one form relative to the other is  $\ln(C_0)/C = k.t$ , i.e., the dependence  $\ln C = f(t, \text{min})$  is linear. Since the concentration of the colored form of the compound is proportional to the absorption (from UV-Vis) and the emission intensity (in fluorescence analysis) in this equation, the concentration can be replaced by the corresponding physical quantity according to the literature [39]. The rate of conversion of the ring-opened form to spirolactam was quantified by calculating the value of the rate constant of the process and half the time using data from the emission spectra of the compounds. The rate constant  $k$  was calculated from the slope of plot of the left side of Equation (2) versus time and the obtained value are summarized in Table 1. The value of the rate constant ( $k$ ) was used to calculate and the  $\tau_{1/2}$ —half time or this is the time for which the current concentration ( $C$ ) of the ring-opened form decreases twice with respect to the initial concentration of ( $C_0$ ), i.e., when  $C = C_0/2$ , then  $t = \tau_{1/2}$ . For a first-order reaction, the value was calculated by the equation:  $\tau_{1/2} = \ln 2/k$  (Table 1) [39]. Moreover, Rh-1 had its maximum absorption band at 565 nm and strongest fluorescence emission at 589 nm in triethylamine solution (Figure 6) and the slowest spirolactam form formation effect ( $k = 4.6 \times 10^{-2} \text{ s}^{-1}$ , Table 1) associated with solution discoloration (Figure 7). In the other compounds, the emission intensities and the value of the rate constant increase in proportion to the increase in the number of methylene groups in the peptide chain (Figures 6 and 7). Stokes shift is an important feature that shows the differences between the structure of the fluorophore in the ground  $S_0$  state and in the first excited state  $S_1$  and was also calculated for the rhodamine peptide derivatives (Figure 6). The Stokes shift of the test compounds are in the range of 721 and 997  $\text{cm}^{-1}$ , which is consistent with rhodamine derivatives known in the literature [40].

The IR spectrum of studied compounds were recorded in KBr tablet ( $\text{KBr}, \text{cm}^{-1}$ ) and shown main characteristic bands, localized at as follow: 3356 ( $\text{N-H}$  stretching vibration ( $\nu_{\text{NH}}$ )), 1701 (s)—NCO (amide) stretching and 1678–1722  $\text{cm}^{-1}$ —a high-intensity peak of  $\nu_{\text{C=O}}$ ; 1511–1528  $\text{cm}^{-1}$  ( $\delta_{\text{NH}}$ ) (Figure 8). As can be seen, the absorption lines in addition prove the functional groups belonging to the structure of the compounds (Figure 8).

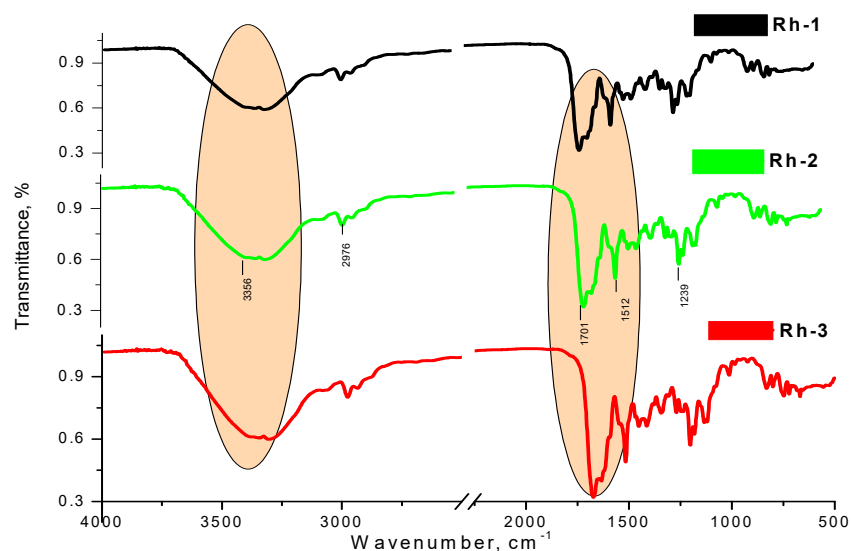


**Figure 8.** IR-spectra of the rhodamine-peptide derivatives.

#### 2.4. Color Characterisation of Cotton Fabrics

CIELab coordinates were used to distinguish the difference in the color of three cotton fabrics dyed with rhodamine-peptides. Figure 9 shows the change in the value of  $a^*$  and  $b^*$  of pristine cotton fabric and the functionalized with chloroacetyl chloride fabrics treated with peptides Rh-1, Rh-2 or Rh-3. The untreated cotton fabric has a white color in daylight with coordinates  $a^*$  and  $b^*$ , approximately equal to zero. For the dyed samples, the color coordinates as an absolute value increase in the order Rh-3 < Rh-1 < Rh-2 and correspond to a red-blue color. The color difference of the fabric compared with untreated fabric changes in the same order. This is in agreement with molar absorption coefficient of the new rhodamine-peptide samples. For all compounds, this coefficient is higher than  $10^4$  which demonstrate a good coloring ability. A better result has been obtained with Rh-2.

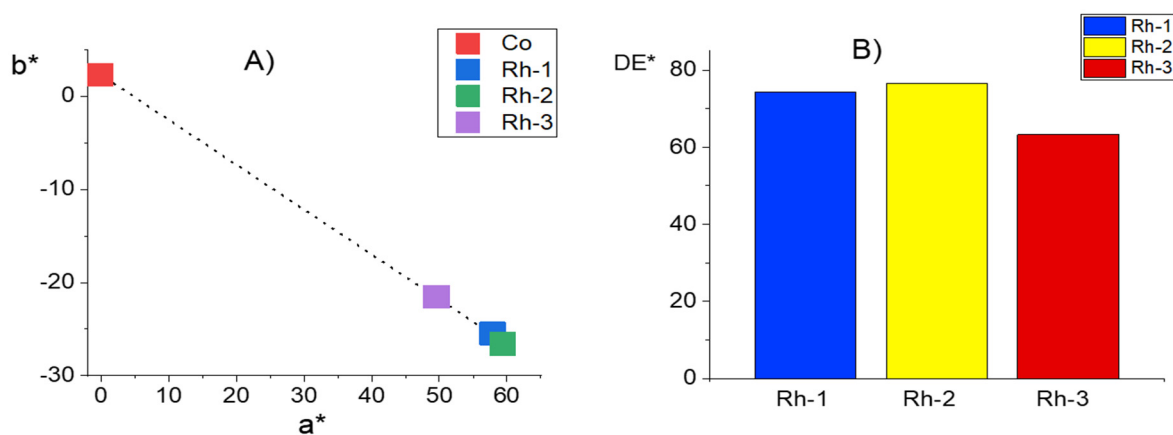


**Figure 9.** Comparison of the colour coordinates of cotton fabric (Co) and fabrics dyed with Rh-1, Rh-2, and Rh-3: (A) color characterization with  $a^*$  and  $b^*$  coordinates; (B) color difference  $DE^*$ .

Figure 10A shows the reflection spectra of the initial cotton fabric and after it dyeing with Rh-1, Rh-2, and Rh-3. The minimum reflectivity ( $R\%$ ) occurs at about 560 nm, where rhodamine peptides have the maximum absorption. As the dyes are fluorescent, there is also a band with a maximum wavelength of 640 nm [41]. Both the minimum and maximum are more pronounced for samples Rh-1 and Rh-2 compared to those of Rh-3. Figure 10B shows the relation of K/S values with the wavelength. The maximum absorbance for the three dyes is 560 nm. The K/S values give information for the dye quantity on the fabric

and its behavior on the textile substrate [42]. It can be seen that the concentrations of the fixed dyes under dyeing conditions are different. Figure 10B shows the relation of K/S values with the wavelength. The maximum absorbance for the three dyes is 560 nm. The K/S values give information for the dye quantity on the fabric and its behavior on the textile substrate. It can be seen that the concentrations of the fixed dyes under dyeing conditions are different. The K/S value is the highest for Rh-2, but the value of Rh-1 is closed to it. The value of Rh-3 is twice as small as Rh-2. The reason for this can be the difference in molecular mass of this rhodamine-peptide and its different behavior in solution.

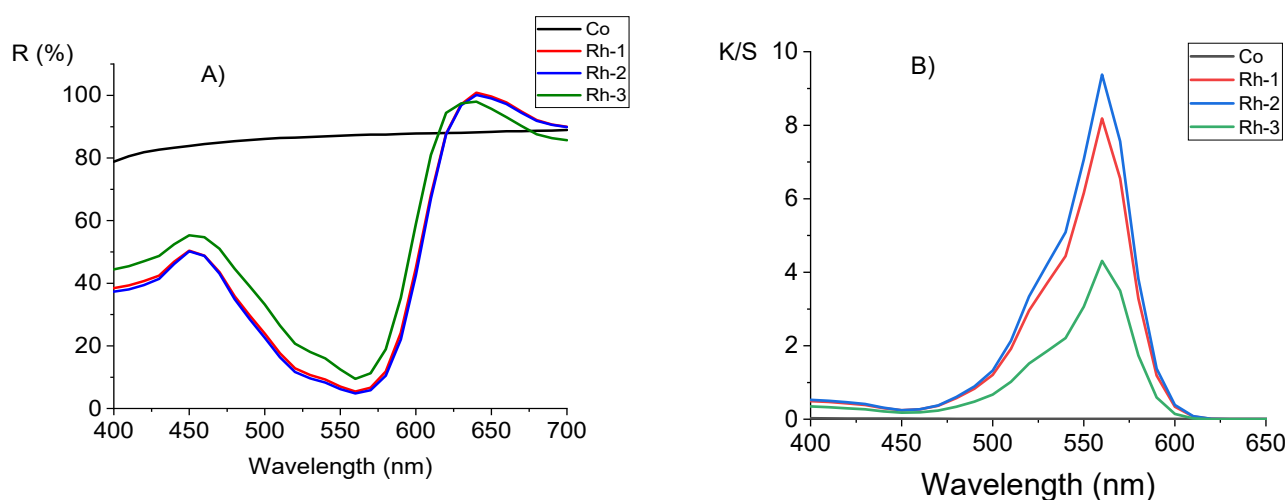


**Figure 10.** Comparison of cotton fabric (Co) and fabrics dyed with Rh-1, Rh-2, and Rh-3: (A) reflection spectra; (B) K/S values in function of wavelength.

### 2.5. Fastness Testing

The stability of the textile material after dyeing with the new antiviral agents was also studied. In order to evaluate the rebinding of the compounds when washing the dyed textile material with soap and water, the spectra of the obtained soap solutions were taken following the washing procedure. When washing the materials with water only, no difference in the spectrum of the solutions after soaking the materials was observed (Figure 11). Studies have shown that in all compounds immediately after washing with soap, the color of the fabric is slightly affected and after drying there is a visible fading of the materials (Figure 11). As can be seen from the figure most strongly absorbs the solution of Rh-2 which can be attributed to a lower binding affinity with the textile material and lower resistance to washing in an alkaline environment. However, no difference was observed in the color of the textiles when soaking the materials in the washing solution (water and soap) for 1 and 24 h.

### 2.6. Virological Activity

Antimicrobial peptides are able to inhibit many pathogens, including Gram-negative and Gram-positive bacteria and fungi. Additionally, some antimicrobial peptides have been shown to have anticancer or antiviral activity, such as indolicidin that has activity toward HIV [43]. Peptides with antiviral activity against influenza can be divided into three main groups. First, entry blocker peptides such as a FluPep that interact with influenza hemagglutinin block its binding to host cells and prevent viral fusion. Second, several peptides display virucidal activity, disrupting viral envelopes (e.g., Melittin). Finally, a third set of peptides interacts with the viral polymerase complex and act as viral replication inhibitors such as PB1 derived peptides [44].

Rhodamine B-conjugated hemorphin-4 analogues demonstrated a virucidal effect against human respiratory syncytial virus (HRSV-S2) and human adenovirus serotype 5 (HAdV-5) for different time intervals (30 and 60 min). The most active is Rh-3 peptide

analogue, which is an analogue of hemorphin-4 containing a rhodamine B residue at the N-terminus and a hydrophobic  $\gamma$ -Abu-Tyr-Pro-Trp-Thr-CONH<sub>2</sub> amino acid sequence of the peptide molecule. The difference between others two compounds is only between one amino acid residues and in particular this is the methylene group (from one to three). Compound Rh-3 showed higher virucidal activity against HRSV-S2 at 60 min, unlike compound Rh-2 which is more active at 30 min. (Table 2). All of the peptides did not show any virucidal activity against HAdV-5 in both 30- and 60-min intervals. Perhaps this is due to the structure of HAdV-5 (non enveloped virus) which do not have lipid bilayer envelope, thus making them more resistant to chemicals.

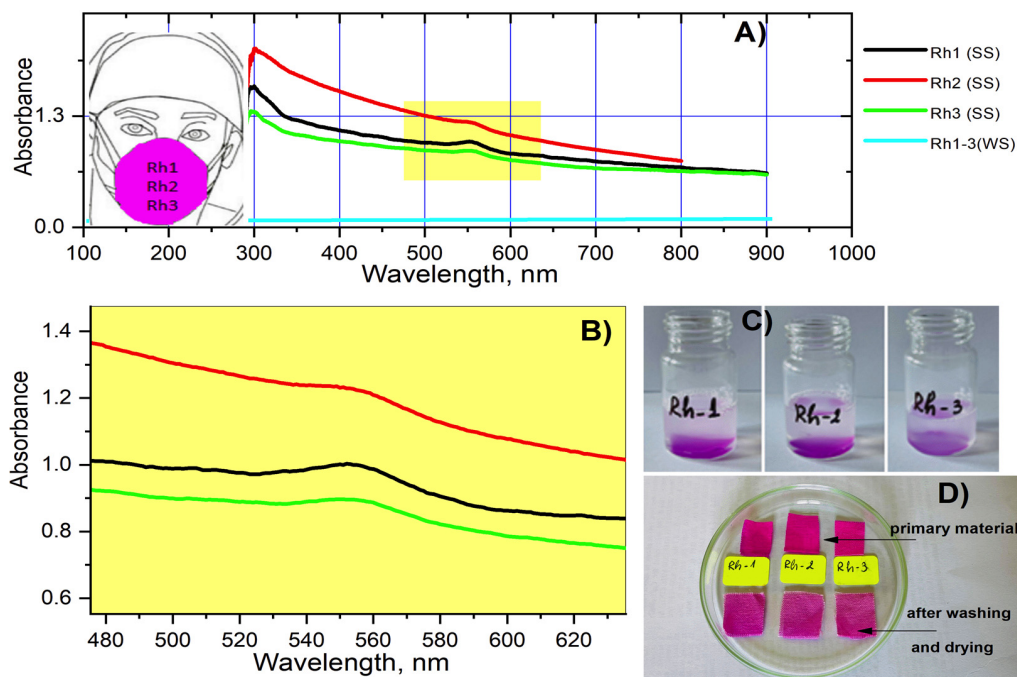


**Figure 11.** UV-Vis (zero) (A) and zoomed at 560 nm (B) spectra of soap (SS) and water (WS) solutions obtained after washing the materials; soap solutions immediately after washing the materials (C); compare the color of the material before and after washing with soap and water. The photos were taken after drying the materials (D).

**Table 2.** Virucidal effect of new rhodamine B-conjugated hemorphin-4 analogues against human respiratory syncytial virus (HRSV-S2) and Human adenovirus serotype 5 (HAdV-5) after 30 min/60 min.

Virus	$\Delta\log$ 30 min			$\Delta\log$ 60 min		
	Rh-1	Rh-2	Rh-3	Rh-1	Rh-2	Rh-3
HRSV-2	0.2	0.4	0.2	1.3	1.3	1.7
HAdV-5	0	0	0	0	0	0

For a more in-depth study of the virucidal effect against both HRSV-S2 and HAdV-5, cotton fabrics dyed with rhodamine-peptides have been also studied. Compared to rhodamine B-conjugated peptides, the virucidal effect of the textile materials was lower. (Table 3). In this case, the virucidal effect of cotton fabrics is due to their direct contact with viruses. The good retention of the tested peptides to the fabric surface does not allow their easy release and reaction with the viruses in solution, which explains the low virucidal activity of the fabrics to the tested viruses.

**Table 3.** Virucidal effect of new cotton fabrics dyed with rhodamine-peptides against human respiratory syncytial virus (HRSV-S2) and human adenovirus C serotype 5 (HAdV-5) after 30 min/60 min.

Virus	$\Delta\log$ 30 min			$\Delta\log$ 60 min		
	Rh-1-Textile	Rh-2-Textile	Rh-3-Textile	Rh-1-Textile	Rh-2-Textile	Rh-3-Textile
HRSV-2	—	—	—	0.2	0.2	0.1
HAdV-5	0	0	0	0	0	0

The newly synthesized rhodamine B-conjugated compounds shown weak virucidal activity. Rh-3 is more potent as opposed to Rh-1 and Rh-2 (see Figures 12 and 13).

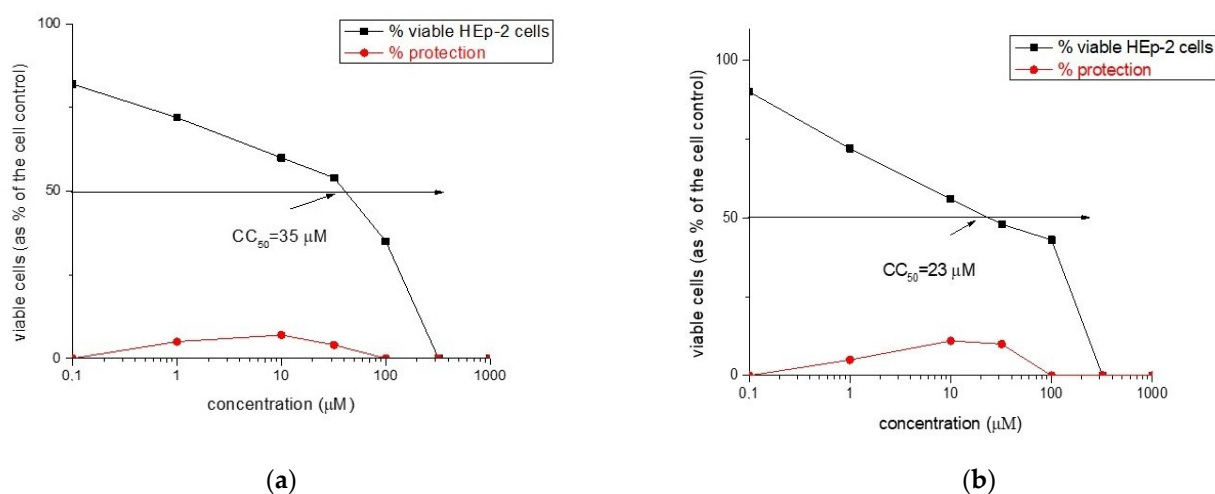


**Figure 12.** Antiviral activity curve (in red) and cytotoxicity curve (in black) of: (a) Rh-1 and (b) Rh-2.

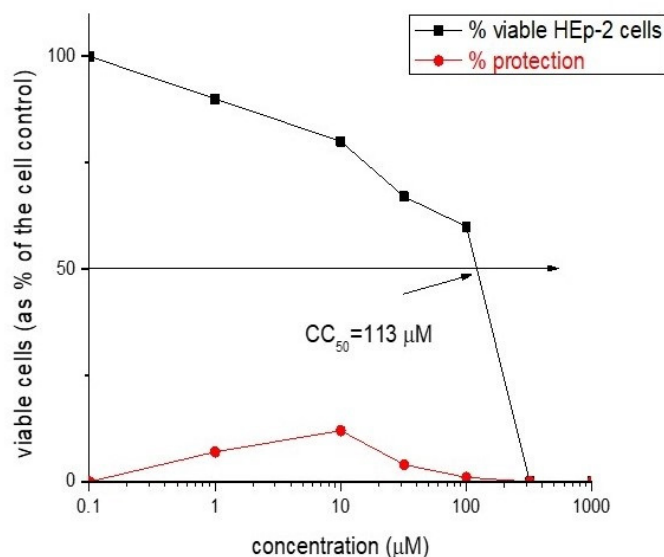


**Figure 13.** Antiviral activity curve (in red) and cytotoxicity curve (in black) activity of Rh-3.

Our experimental data suggest that in the new hybrid peptide compounds containing a rhodamine B residue, not only the position of the modification but also the nature and length of the amino acid sequence leads to significant changes in peptide activity and affinity. The results suggest that incorporation of different amino acids at the N-terminus of the hemorphin-4 scaffold deserve further evaluation in antiviral and virucidal effects.

The cytotoxicity data and antiviral activity of the compounds against human respiratory syncytial virus (HRSV-S2) and human adenovirus C serotype 5 (HAdV-5) in HEp-2 cell culture are shown in Table 4.

**Table 4.** Cytotoxicity and antiviral activity of new rhodamine-peptides against human respiratory syncytial virus (HRSV-S2) and Human adenovirus C serotype 5 (HAdV-5) in HEp-2 cell culture.

Compound	Cytotoxicity		Antiviral Activity		
	CC <sub>50</sub> (μM/mL) in HEp-2 Cells	HRSV-S2		HAdV-5	
		IC <sub>50</sub> (μM/mL)	SI	IC <sub>50</sub> (μM/mL)	SI
Rh-1	35	NA	-	NA	-
Rh-2	23	NA	-	NA	-
Rh-3	113	NA	-	NA	-

### 3. Materials and Methods

#### 3.1. Synthesis of the Peptides (Rh-1, Rh-2, and Rh-3)

All reagents and solvents were analytical or HPLC grade and were bought from Fluka or Merck, and used without further purification. The protected amino acids and Fmoc (9-fluorenylmethoxycarbonyl)-Rink Amide MBHA (4-methylbenzhydramine) Resin were purchased from Iris Biotech (Germany). The 3-functional amino acids were embedded as follows: Tyr—as N<sup>α</sup>-Fmoc-Tyr(tBu)-OH, Thr—as N<sup>α</sup>-Fmoc-Thr(tBu)-OH, and Trp—as N<sup>α</sup>-Fmoc-Trp(Boc)-OH.

The solid-phase peptide synthesis by Fmoc chemistry was used to obtain new rhodamine B-conjugated hemorphin-4 analogues. The Fmoc-Rink-Amide MBHA resin was used as solid phase carrier to obtain the C-terminal amide derivatives and 2-(1H-benzotriazole-1-yl)-1,1,3,3-tetramethylammonium tetrafluoroborate (TBTU) was used as a coupling reagent. The coupling reactions were performed using for amino acid/TBTU/HOBt/DIPEA/resin a molar ratio of 3/2.9/3/6/1, in a 1:1 mixture of DMF/DCM. A 20% piperidine solution in N,N-dimethylformamide (DMF) was used to remove the Fmoc group at every step. After each reaction step, the resin was washed with DMF (3 × 1 min), isopropyl alcohol (3 × 1 min) and CH<sub>2</sub>Cl<sub>2</sub> (3 × 1 min). The coupling and deprotection reactions were checked by the Kaiser test [45,46]. The cleavage of the synthesized peptide from the resin was done, using a mixture of 95% trifluoroacetic acid (TFA), 2.5% triisopropylsilan (TIS) and 2.5% water. The peptide was obtained as a filtrate in TFA and precipitated with cold, dry ether. The precipitate was filtered, dissolved in water and lyophilized to yield the compounds as a powder. The crude peptides were dissolved in H<sub>2</sub>O and acetonitrile was added until complete dissolving was observed. The peptides were obtained as white powders with a purity of >97% as determined by analytical HPLC. The structures were confirmed by high-resolution electrospray mass spectrometry. The purity of the peptides was monitored on a reversed-phase high-performance liquid chromatography (RP-HPLC), column: SymmetryShield<sup>TM</sup> RP-18, 3.5μ, (50 × 4.6 mm), flow: 1 mL/min, H<sub>2</sub>O (0.1% TFA)/CH<sub>3</sub>CN (0.1% TFA), gradient 0→100% (45 min) and 100% (5 min). The crude peptides were purified using semi-preparative HPLC, column XBridge<sup>TM</sup> Prep C18 10 μm (10 × 250 mm), flow: 5 mL/min, H<sub>2</sub>O (0.1% TFA)/CH<sub>3</sub>CN (0.1% TFA), gradient 20→100% (50 min). The analytical data for the synthesized peptides (Supplementary Materials) prepared were as follows: compound Rh-1 *t<sub>R</sub>* 25.90 min, 1045.5062 calculated [M + H<sup>+</sup>], 1046.5051 observed [M + H<sup>+</sup>]; compound Rh-2 *t<sub>R</sub>* 26.60 min, 1059.5218 calculated [M + H<sup>+</sup>], 1060.5421 observed [M + H<sup>+</sup>]; compound Rh-3 *t<sub>R</sub>* 27.20 min, 1073.5375 calculated [M + H<sup>+</sup>], 1074.5581 observed [M + H<sup>+</sup>]. The rhodamine B-conjugated hemorphin-4 analogues were checked by optical rotation in methanol (*c* = 0.01) at 20 °C, [α]<sub>589</sub><sup>20</sup> as follows: compound Rh-1—40°, compound Rh-2—34°, compound Rh-3—48°.

### 3.2. Physicochemical Characterization

#### 3.2.1. Spectral Measurements

“Varian-Cary” Spectrophotometer has been used for UV-vis spectrophotometric measurements. The fluorescence spectra were recorded on a Perkin Elmer LS55 spectrophotometer at the same concentrations. The concentrations of the compounds in the triethylamine and double distilled water spectral solutions are as follows: Rh-1:  $C = 4.09 \times 10^{-5} \text{ mol L}^{-1}$ ; Rh-2:  $C = 3.63 \times 10^{-5} \text{ mol L}^{-1}$ ; Rh-3:  $C = 3.98 \times 10^{-5} \text{ mol L}^{-1}$ . All used reagent were analytical grade. The kinetic data for the degree of open/closed of spiro lactam ring were obtained according to Equations (1) and (2) and the rate constant  $k$  was fitted by Equation (2) (open  $\rightarrow$  close of the ring) taking into account first-order of the reactions [39]:

$$\ln(I_0/I_t) = k.t \quad (1)$$

$$\ln\left(\frac{I_\infty - I_0}{I_\infty - I_t}\right) = k.t \quad (2)$$

where  $(I_0)$ ,  $(I_t)$ , and  $(I_\infty)$  refer to the signal proportional to the initial-, time  $t$ -, and final intensity of emission, respectively.

The IR spectrum was recorded in potassium bromide (KBr) pellet with a Varian 660 FTIR spectrophotometer the spectra in the  $4000\text{--}500 \text{ cm}^{-1}$  range using a Fourier Transform Infrared Spectroscopy (FT-IR). The sample was scanned 256 times with a resolution of  $2 \text{ cm}^{-1}$ . The molecular mass and purity of the compound was confirmed by high-resolution electrospray mass spectrometry on a Q Exactive high-resolution mass spectrometer (Thermo Fisher Scientific Inc., San Jose, CA, USA) equipped with TurboFlow TM Transcend chromatography system (Thermo Fisher Scientific Inc., San Jose, CA, USA) and heated electrospray ionization (HESI II) source. Data acquisition and processing were done by XCalibur<sup>®</sup> 2.4 software (Thermo Fisher Scientific Inc., San Jose, CA, USA). The instrumental parameters were as follows: Spray Voltage—4.0 KV, Sheath Gas—30 AU, Auxiliary Gas—12 AU, Capillary Temperature—300 °C, Spare Gas—3 AU, Heater Temperature—300 °C. Full scan experiments were carried out in a range of  $120\text{--}2000 \text{ m/z}$  at 140,000 resolution.

Optical rotations were recorded on an MCP200 modular circular polarimeter (Anton Paar Opto Tec GmbH, Seelze, Germany).

#### 3.2.2. Potentiometric Titration

A digital pH-meter (Jenway) was used for potentiometric titrations of the compounds in order to determinate  $pK_a$  and  $pI$  values. For each titration, 5.00 mL from stock water solutions of the rhodamine derivatives were titrated with standardized base ( $0.0112 \text{ mol L}^{-1} \text{ NaOH}$ ). Data (volume of titrant vs. pH) were processed by Origin8Pro software for determination of  $pK_a$  of the sample.

### 3.3. Cotton Fabric Modification and Characterization

#### 3.3.1. Functionalization of Cotton Fabric with Chloroacetyl Chloride

Cotton fabric ( $140 \text{ g/m}^2$ ) was modified with 10% ( $v/v$ ) chloroacetyl chloride ( $\text{ClCOCH}_2\text{Cl}$ ) in  $N,N$ -dimethylformamide at 25 °C for 2 h. The solution was of liquor to goods ratio of 20:1. Then the fabric has been removed from the solution, washed thoroughly with water, and dried in the open air [47].

#### 3.3.2. Dyeing of Functionalized Cotton Fabric with Rh-1, Rh-2, and Rh-3

The dyeing solution of rhodamine-peptide derivatives were prepared by dissolving each dye in DMF and water (the ratio 1:14.5). The modified with chloroacetyl chloride cotton fabric was impregnated with relevant dye solution (2.0 owf %) at a liquor to goods ratio 5:1, and then dried at room temperature for 30 min and at 50 °C for 60 min. The colored cotton fabric has been washed thoroughly with water.

### 3.3.3. Characterization of Cotton Fabrics

The color coordinates ( $L^* a^* b^*$ ) and the reflectance spectra ( $R\%$ ) of dyed cotton fabrics have been determined by using Datacolor Spectraflash SF300 spectrophotometer (Datacolor, NJ, USA) and Micromatch 2000<sup>®</sup> software. The samples were measured under illuminant D65 using the 10° standard observer. A non-treated cotton fabric has been used for the color difference quantification [48].

For the assessment of the depth of color and the obtained shade from rhodamine-peptides the Kubelka–Munk theory and Equation (3) has been applied.

$$K/S = (1 - R_\lambda)^2 / 2 \cdot R_\lambda \quad (3)$$

where  $K$  is the light absorption coefficient,  $S$  is the light scattering coefficient, and  $R_\lambda$  is the reflectance of a dyed fabric.

### 3.3.4. Fastness Testing

The dyed fabrics were tested for colorfastness at washed with water and with soap water solution of the dyed material following standard procedures given in [49]. The UV-Vis spectra recording and monitored the absorption at  $\lambda = 561$  nm corresponding to the analytical signal of the peptide derivatives on the solutions after washing of the fabric, immediately and after 1 and 24 h were carried out. The soap solutions were pre-diluted twice with d.H<sub>2</sub>O and filtered through a paper filter to measure the absorbed radiation.

## 3.4. Virology

### 3.4.1. Cytotoxicity Assay

Inoculation of monolayer cells in 96-well plates (Costar<sup>®</sup>, Corning Inc., Kennebunk, ME, USA) was performed with 0.1 mL/well-containing concentrations of the compounds diluted in a maintenance medium. Cells were incubated in a humidified atmosphere at 37 °C and 5% CO<sub>2</sub> for 48 h. After microscopic evaluation, the maintenance medium containing the test compound was removed, cells were washed, and 0.1 mL of maintenance medium supplemented with 0.005% neutral red dye was added to each well, and cells were incubated at 37 °C for 3 h. After incubation, the neutral red day was removed, and cells were washed once with PBS, and 0.15 mL/well desorb solution (1% glacial acetic acid and 49% ethanol in distilled water) was added. The optical density (OD) of each well was read at 540 nm in a microplate reader (Biotek Organon, West Chester, PA, USA). The 50% cytotoxic concentration (CC<sub>50</sub>) was defined as the material concentration that reduced the cell viability by 50% when compared to untreated control.

### 3.4.2. Antiviral Activity Assay

Antiviral screening was based on the viral yield reduction technique. Cytopathic effect (CPE) inhibition test used confluent cell monolayer in 96-well plates infected with 100 CCID<sub>50</sub> in 0.1 mL. After 1 h of virus adsorption, the extract was added in various concentrations and cells were incubated for 48 h at 37 °C. The viable cells were stained according to the neutral red uptake procedure and the percentage of CPE inhibition for each concentration of the test sample was calculated using the following formula: % CPE =  $[\text{OD}_{\text{test sample}} - \text{OD}_{\text{virus control}}] / [\text{OD}_{\text{toxicity control}} - \text{OD}_{\text{virus control}}] \times 100$ , where  $\text{OD}_{\text{test sample}}$  is the mean value of the ODs of the wells inoculated with virus and treated with the test sample in the respective concentration,  $\text{OD}_{\text{virus control}}$  is the mean value of the ODs of the virus control wells (with no compound in the medium) and  $\text{OD}_{\text{toxicity control}}$  is the mean value of the ODs of the wells not inoculated with virus but treated with the corresponding concentration of the test sample. The 50% inhibitory concentration (IC<sub>50</sub>) was defined as the concentration of the material that inhibited 50% of viral replication when compared to the virus control. The selectivity index (SI) was calculated from the ratio CC<sub>50</sub>/IC<sub>50</sub>.

### 3.4.3. Virucidal Assay

Samples of 1 mL, containing human respiratory syncytial virus (HRSV-S2) (105,3 CCID50) or respectively human adenovirus type 5 (HAdV5) (106,3 CCID50), and tested compound in its maximum tolerable concentration (MTC) were contacted in a 1:1 ratio and subsequently stored at room temperature for different time intervals (30 and 60 min). Then, the residual infectious virus content in each sample was determined by the end-point dilution method, and  $\Delta I_{gs}$  as compared to the untreated controls were evaluated.

Our approach to this test for virocidal effect of fabrics dyed with Rh-1, Rh-2 and Rh-3 was to cut identical pieces of the textiles (1 cm<sup>2</sup>) and immerse them in a viral suspension (100  $\mu$ L) for the respective times (30 and 60 min). We used non dyed textiles of the same material for the control. The virus suspension was recovered by exhaustion after the appropriate time has elapsed. The residual infectious virus content was determined by the end-point dilution method followed by evaluation of  $\Delta I_{gs}$  through comparison between each sample and control.

## 4. Conclusions

A systematic study of three novel rhodamine-peptide derivatives for textile dyeing has been presented. A modified with chloroacetyl chloride cotton fabric was used, which facilitated the deposition and retention of the new compounds. An intense and even color with good moisture resistance is obtained. A slight difference in the color characteristics of the tissues was found by colorimetric analysis. By using combined experimental approaches, the structural-textile application has been investigated by UV-Vis and fluorometric methods. Antiviral and virucidal activities of both the peptide-rhodamine B compounds and the dyed textile material were also studied. The most potent is Rh-3 peptide analogue, which is an analogue of hemorphin-4 containing a rhodamine B residue at the N-terminus and a hydrophobic  $-\gamma$ -Abu-Tyr-Pro-Trp-Thr-CONH<sub>2</sub> amino acid sequence of the peptide molecule. Spectral studies have shown that the color of the aqueous solutions of compounds depends on their structural behavior and the type of solvent. In a polar protic solvent such as water, regardless of the pH of the medium, the compounds showed stability of ring-opened form and fluorescence on of the compounds without being affected by the number of methylene groups in the structure of the peptide moiety. The steric effect is more pronounced in the aprotic solvent of the compounds and the effect depends on the type of peptide chain. These structural characteristics are directly related to the dyeing of textile materials.

**Supplementary Materials:** The following are available online, Figure S1. ESI-MS spectrum of Rh-1; Figure S2. ESI-MS spectrum of Rh-2; Figure S3. ESI-MS spectrum of Rh-3.

**Author Contributions:** Conceptualization, P.T., S.G. and D.S.; methodology, P.T., S.G. and D.S.; software, S.G. and P.T.; formal analysis, P.T., S.G., P.P., D.S., I.G., P.G. and I.N.; investigation, P.T., S.G., P.P., D.S., I.G., P.G. and I.N.; writing—original draft preparations, P.T., S.G. and D.S.; writing—review and editing—P.T., S.G., D.S. and I.G.; visualization, P.T., S.G. and D.S.; project administration, P.T. All authors have read and agreed to the published version of the manuscript.

**Funding:** This research was funded by Bulgarian National Scientific Fund project KII-06-ДК1/11 of the Ministry of Education and Science, Bulgaria.

**Institutional Review Board Statement:** Not applicable.

**Informed Consent Statement:** Not applicable.

**Data Availability Statement:** Data is contained within the article or Supplementary Material.

**Acknowledgments:** This work was financial supported by the Bulgarian National Scientific Fund project KII-06-ДК1/11 (title: "Textile materials to prevent the spread of SARS-CoV2 and other pathogens") of the Ministry of Education and Science, Bulgaria.

**Conflicts of Interest:** The authors declare no conflict of interest.

**Sample Availability:** Samples of the compounds are available from the authors.

## References

1. Jamison, J.M.; Krabill, K.; Hatwalkar, A.; Jamison, E.; Tsai, C.C. Potentiation of the antiviral activity of poly r (AU) by xanthene dyes. *Cell Biol. Int. Rep.* **1990**, *14*, 1075–1084. [[CrossRef](#)]
2. Lavis, L.D.; Raines, R.T. Bright ideas for chemical biology. *ACS Chem. Biol.* **2008**, *3*, 142–155. [[CrossRef](#)] [[PubMed](#)]
3. Li, M.; Yuan, L.; Chen, Y.; Ma, W.; Ran, F.; Zhang, L.; Zhou, D.; Xiao, S. Rhodamine B-based fluorescent probes for molecular mechanism study of the anti-influenza activity of pentacyclic triterpenes. *Eur. J. Med. Chem.* **2020**, *205*, 112664. [[CrossRef](#)]
4. Hwaná Kwak, J.; He, Y.; Yoon, B.; Juá Kang, E.; Koo, S.; Yang, Z.; Kang, E.J.; Lee, B.H.; Han, S.-Y.; Yoo, Y.C.; et al. Synthesis of rhodamine-labelled dieckol: Its unique intracellular localization and potent anti-inflammatory activity. *Chem. Commun.* **2014**, *50*, 13045–13048. [[CrossRef](#)]
5. Beija, M.; Afonso, C.A.; Martinho, J.M. Synthesis and applications of Rhodamine derivatives as fluorescent probes. *Chem. Soc. Rev.* **2009**, *38*, 2410–2433. [[CrossRef](#)]
6. Birtalan, E.; Rudat, B.; Kölmel, D.K.; Fritz, D.; Vollrath, S.B.; Schepers, U.; Bräse, S. Investigating rhodamine B-labeled peptoids: Scopes and limitations of its applications. *Pept. Sci.* **2011**, *96*, 694–701. [[CrossRef](#)] [[PubMed](#)]
7. Cagno, V.; Tintori, C.; Civra, A.; Cavalli, R.; Tiberi, M.; Botta, L.; Brai, A.; Poli, G.; Tapparel, C.; Lembo, D.; et al. Novel broad spectrum virucidal molecules against enveloped viruses. *PLoS ONE* **2018**, *13*, e0208333. [[CrossRef](#)]
8. Carravilla, P.; Cruz, A.; Martin-Ugarte, I.; Oar-Arteta, I.R.; Torralba, J.; Apellaniz, B.; Pérez-Gil, J.; Requejo-Isidro, J.; Huarte, N.; Nieva, J.L. Effects of HIV-1 gp41-derived virucidal peptides on virus-like lipid membranes. *Biophys. J.* **2017**, *113*, 1301–1310. [[CrossRef](#)] [[PubMed](#)]
9. Pazos, E.; Vazquez, O.; Mascarenas, J.L.; Vazquez, M.E. Peptide-based fluorescent biosensors. *Chem. Soc. Rev.* **2009**, *38*, 3348–3359. [[CrossRef](#)]
10. Wang, L.; Xie, J.; Schultz, P.G. Expanding the genetic code. *Annu. Rev. Biophys. Biomol. Struct.* **2006**, *35*, 225–249. [[CrossRef](#)]
11. Thurley, S.; Röglin, L.; Seitz, O. Hairpin peptide beacon: Dual-labeled PNA-peptide-hybrids for protein detection. *J. Am. Chem. Soc.* **2007**, *129*, 12693–12695. [[CrossRef](#)]
12. Chersi, A.; Giommi, S.; Rosanò, L. Selective ‘in synthesis’ labeling of peptides with biotin and rhodamine. *Biochim. Biophys. Acta Gen. Subj.* **2000**, *1474*, 196–200. [[CrossRef](#)]
13. Blishchenko, E.Y.; Sazonova, O.V.; Kalinina, O.A.; Yatskin, O.N.; Philippova, M.M.; Surovoy, A.Y.; Karelina, A.A.; Ivanov, V.T. Family of hemorphins: Co-relations between amino acid sequences and effects in cell cultures. *Peptides* **2002**, *23*, 903–910. [[CrossRef](#)]
14. Jinsmaa, Y.; Yoshikawa, M. Release of Hemorphin-5 from Human Hemoglobin by Pancreatic Elastase. *Biosci. Biotechnol. Biochem.* **2002**, *66*, 1130–1132. [[CrossRef](#)]
15. Ali, A.; Alzeyoudi, S.A.R.; Almutawa, S.A.; Alnajjar, A.N.; Vijayan, R. Molecular basis of the therapeutic properties of hemorphins. *Pharmacol. Res.* **2020**, *158*, 104855. [[CrossRef](#)]
16. Ayoub, M.A.; Vijayan, R. Hemorphins Targeting G. Protein-Coupled Receptors. *Pharmaceuticals* **2021**, *14*, 225. [[CrossRef](#)] [[PubMed](#)]
17. Wei, F.; Zhao, L.; Jing, Y. Hemoglobin-derived peptides and mood regulation. *Peptides* **2020**, *127*, 170268. [[CrossRef](#)] [[PubMed](#)]
18. Mielczarek, P.; Hartman, K.; Drabik, A.; Hung, H.Y.; Huang, E.Y.; Gibula-Tarlowska, E.; Kotlinska, J.H.; Silberring, J. Hemorphins—From discovery to functions and pharmacology. *Molecules* **2021**, *26*, 3879. [[CrossRef](#)] [[PubMed](#)]
19. Yang, Y.R.; Chiu, T.H.; Chen, C.L. Structure-activity relationships of naturally occurring and synthetic opioid tetrapeptides acting on locus coeruleus neurons. *Eur. J. Pharmacol.* **1999**, *372*, 229–236. [[CrossRef](#)]
20. Todorov, P.; Peneva, P.; Pechlivanova, D.; Georgieva, S.; Dzhambazova, E. Synthesis, characterization and nociceptive screening of new VV-hemorphin-5 analogues. *Bioorg. Med. Chem. Lett.* **2018**, *28*, 3073–3079. [[CrossRef](#)] [[PubMed](#)]
21. Todorov, P.; Rangelov, M.; Peneva, P.; Todorova, N.; Tchekalarova, J. Anticonvulsant evaluation and docking analysis of VV-Hemorphin-5 analogues. *Drug Dev. Res.* **2019**, *80*, 425–437. [[CrossRef](#)] [[PubMed](#)]
22. Todorov, P.; Peneva, P.; Georgieva, S.; Tchekalarova, J.; Vitkova, V.; Antonova, K.; Georgiev, A. Synthesis, characterization and anticonvulsant activity of new azobenzene-containing VV-hemorphin-5 bio photoswitch. *Amino Acids* **2019**, *51*, 549–563. [[CrossRef](#)] [[PubMed](#)]
23. Todorov, P.; Peneva, P.; Tchekalarova, J.; Rangelov, M.; Georgieva, S.; Todorova, N. Synthesis, characterization and anticonvulsant activity of new series of N-modified analogues of VV-hemorphin-5 with aminophosphonate moiety. *Amino Acids* **2019**, *51*, 1527–1545. [[CrossRef](#)] [[PubMed](#)]
24. Todorov, P.; Peneva, P.; Tchekalarova, J.; Georgieva, S. Potential anticonvulsant activity of novel VV-hemorphin-7 analogues containing unnatural amino acids: Synthesis and characterization. *Amino Acids* **2020**, *52*, 567–585. [[CrossRef](#)] [[PubMed](#)]
25. Todorov, P.; Georgieva, S.; Peneva, P.; Tchekalarova, J. Spectral and electrochemical solvatochromic investigations of newly synthesized peptide-based chemosensor bearing azobenzene side chain bio photoswitch. *Dyes Pigm.* **2021**, *191*, 109348. [[CrossRef](#)]
26. Guo, P.; Wang, Y.; Zhuang, Q. Highly sensitive and selective biosensor for heparin detection with rhodamine B-labelled peptides as fluorescent bioreceptors. *Sens. Actuators. B Chem.* **2019**, *299*, 126873. [[CrossRef](#)]
27. Ali, A.; Baby, B.; Soman, S.S.; Vijayan, R. Molecular insights into the interaction of hemorphin and its targets. *Sci. Rep.* **2019**, *9*, 1–6. [[CrossRef](#)]
28. Ni, W.; Yang, X.; Yang, D.; Bao, J.; Li, R.; Xiao, Y.; Hou, C.; Wang, H.; Liu, J.; Yang, D.; et al. Role of angiotensin-converting enzyme 2 (ACE2) in COVID-19. *Crit. Care* **2020**, *24*, 422. [[CrossRef](#)]

29. Srivastava, N.; Garg, P.; Srivastava, P.; Seth, P.K. A molecular dynamics simulation study of the ACE2 receptor with screened natural inhibitors to identify novel drug candidate against COVID-19. *Peer J.* **2021**, *9*, e11171. [[CrossRef](#)] [[PubMed](#)]
30. Sauperl, O. Textiles for protection against microorganism. *AIP Conf. Proc.* **2016**, *1727*, 020021. [[CrossRef](#)]
31. Iyigundogdu, Z.U.; Demir, O.; Asutay, A.B.; Sahin, F. Developing novel antimicrobial and antiviral textile products. *Appl. Biochem. Biotechnol.* **2017**, *181*, 1155–1166. [[CrossRef](#)] [[PubMed](#)]
32. Pizzorno, A.; Abed, Y.; Boivin, G. Influenza drug resistance. *Semin. Respir. Crit. Care Med.* **2011**, *32*, 409–422. [[CrossRef](#)] [[PubMed](#)]
33. Alavi, M. Modifications of microcrystalline cellulose (MCC), nanofibrillated cellulose (NFC), and nanocrystalline cellulose (NCC) for antimicrobial and wound healing applications. *e-Polymers* **2019**, *19*, 103–119. [[CrossRef](#)]
34. Stevenazzi, A.; Marchini, M.; Sandrone, G.; Vergani, B.; Lattanzio, M. Amino acidic scaffolds bearing unnatural side chains: An old idea generates new and versatile tools for the life sciences. *Bioorg. Med. Chem. Lett.* **2014**, *24*, 5349–5356. [[CrossRef](#)]
35. Fornander, L.H.; Feng, B.; Beke-Somfai, T.; Nordén, B. UV transition moments of tyrosine. *J. Phys. Chem. B* **2014**, *118*, 9247–9257. [[CrossRef](#)] [[PubMed](#)]
36. Yashchuk, V.M.; Kudrya, V.Y.; Levchenko, S.M.; Tkachuk, Z.Y.; Hovorun, D.M.; Mel'nik, V.I.; Vorob'yov, V.P.; Klishevich, G.V. Optical response of the polynucleotides-proteins interaction. *Mol. Cryst. Liq. Cryst.* **2011**, *535*, 93–110. [[CrossRef](#)]
37. Xia, M.C.; Cai, L.; Zhang, S.; Zhang, X. Cell-penetrating peptide spirolactam derivative as a reversible fluorescent pH probe for live cell imaging. *Anal. Chem.* **2017**, *89*, 1238–1243. [[CrossRef](#)] [[PubMed](#)]
38. Mayer, U.; Oberlinner, A. Rhodamine dyes. U.S. Patent 4647675, 3 March 1987.
39. El Seoud, O.A.; Baader, W.J.; Bastos, E.L. Practical chemical kinetics in solution. In *Encyclopedia of Physical Organic Chemistry*; Wiley: Hoboken, NJ, USA, 2016; Volume 21, pp. 1–68. [[CrossRef](#)]
40. Zheng, H.; Shang, G.-Q.; Yang, S.-Y.; Gao, X.; Xu, J.-G. Fluorogenic and chromogenic rhodamine spirolactam based probe for nitric oxide by spiro ring opening reaction. *Org. Lett.* **2008**, *10*, 2357–2360. [[CrossRef](#)] [[PubMed](#)]
41. Staneva, D.; Grabchev, I.; Betcheva, R. Sensor potential of 1, 8-naphthalimide and its dyeing ability of cotton fabric. *Dyes Pigm.* **2013**, *98*, 64–70. [[CrossRef](#)]
42. Becerir, B. An approach for estimating the relation between K/S values and dye uptake. *Colourage* **2003**, *50*, 39–48.
43. Robinson, W.E., Jr.; McDougall, B.; Tran, D.; Selsted, M.E. Anti-HIV-1 activity of indolicidin, an antimicrobial peptide from neutrophils. *J. Leukoc. Biol.* **1998**, *63*, 94–100. [[CrossRef](#)] [[PubMed](#)]
44. Skalickova, S.; Heger, Z.; Krejcová, L.; Pekarík, V.; Bastl, K.; Janda, J.; Kostolansky, F.; Vareckova, E.; Zitka, O.; Adam, V.; et al. Perspective of use of antiviral peptides against influenza virus. *Viruses* **2015**, *7*, 5428–5442. [[CrossRef](#)] [[PubMed](#)]
45. Kaiser, E.; Colescott, R.L.; Bossinger, C.D.; Cook, P.I. Color test for detection of free terminal amino groups in the solid-phase synthesis of peptides. *Anal. Biochem.* **1970**, *34*, 595–598. [[CrossRef](#)]
46. Sarin, V.K.; Kent, S.B.H.; Tam, J.P.; Merrifield, R.B. Quantitative monitoring of solid-phase peptide synthesis by the ninhydrin reaction. *Anal. Biochem.* **1986**, *117*, 147–157. [[CrossRef](#)]
47. Staneva, D.; Vasileva-Tonkova, E.; Grabchev, I. Chemical modification of cotton fabric with 1, 8-naphthalimide for use as heterogeneous sensor and antibacterial textile. *J. Photochem. Photobiol. A Chem.* **2019**, *382*, 111924. [[CrossRef](#)]
48. Becerir, B. Color concept in textiles: A review. *J. Text. Eng. Fashion Technol.* **2017**, *1*, 240–244. [[CrossRef](#)]
49. Mohini, K.; Tejashree, L.; Vijay, N. Data set on analysis of dyeing property of natural dye from *Thespesia populnea* bark on different fabrics. *Data Brief* **2018**, *16*, 401–410. [[CrossRef](#)]